



Supramolecular Assembly of Poly(ionic liquid) Nanogel Driven By Host-Stabilized Charge Transfer Interaction

Yuntao Tang,¹ Ke Wang,¹ Yong Zuo,² Xi Chen,² Yubing Xiong ,^{1,2} Yumin Yuan¹

¹Department of Chemistry, Zhejiang Sci-Tech University, Hangzhou 310018, Zhejiang Province, China

²College of Chemistry and Chemical Engineering, Northwest Normal University, Lanzhou 730070, China

Correspondence to: Y. Xiong (E-mail: yubing_xiong@163.com), Y. Yuan (E-mail: yuan42@hotmail.com)

Received 30 July 2019; Revised 18 September 2019; accepted 19 September 2019

DOI: 10.1002/pola.29516

ABSTRACT: Poly(ionic liquid) (PIL)-based nanogels, functionalized by naphthyl (Np), are fabricated via a facile one-step ternary crosslinking copolymerization in selective solvent. The size of PIL nanogels can be conveniently regulated through the feed ratio of IL monomer to crosslinker. The presence of Np groups in PIL nanogel is confirmed by using ultraviolet–visible (UV–vis), Fourier transform infrared, and X-ray photoelectron spectroscopy measurements. Through introducing cucurbit[8]uril (CB[8]) and bisviologen compound (DEDV) as the host molecule and electron acceptor, respectively, host-stabilized charge transfer (HSCT) interaction is achieved through utilizing Np containing PIL nanogel as the building block. The studies reveal that PIL nanogels can form

schistose aggregates in the scale of micrometer via HSCT interaction. The aggregates will be broken in the presence a competitive guest molecule (amantadine) and can recover by adding another host molecule (CB[7]). HSCT interaction among CB[8], DEDV and PIL nanogel is investigated by dynamic light scattering, UV–vis, and Proton nuclear magnetic resonance. Our studies thus provided an applicable strategy for constructing dynamic polymer nanoparticles through noncovalent interaction. © 2019 Wiley Periodicals, Inc. *J. Polym. Sci., Part A: Polym. Chem.* **2019**

KEYWORDS: charge transfer interaction; nanogel; poly(ionic liquid); supramolecular assembly

INTRODUCTION Noncovalent interactions between different building blocks can allow the self-assembly behaviors with reversibility and versatile stimuli responses. Supramolecular self-assembly mediated by non-covalent interactions thus has attracted tremendous interests in the fields of polymer, smart material, life science, and so forth.^{1–3} Till now, the most widely developed noncovalent interactions include hydrogen bonding, hydrophobic interaction, host–guest interaction, electrostatic interaction, π – π stacking, coordination, and so on.^{4–7} These noncovalent interactions can endow the organized systems with micro/macrotransformation in response to external stimuli, such as temperature, light, pH, magnetic field, electricity, and compounds, which have found many potential applications in biomimetic material, controlled drug delivery, actuators, and sensors.^{8–11}

Through host-stabilized charge transfer (HSCT) interaction, more than one guest molecule can be accommodated into the host molecule. Additionally, the as-formed complex can produce a confined environment, which benefits to get insight into the new form of stereoisomerism, bimolecular reaction, and molecular recognition.^{12,13} In the past two decades, cucurbit[n]urils (CB[n]) have been popular host compounds used as the building elements in view of their symmetrical

pumpkin shape.^{14,15} Especially, CB[8] can form stable 1:1:1 ternary complexes, in which the donor and the acceptor are both encapsulated in its cavity. The short distance between the donor and the acceptor can enhance the CT interaction greatly.^{16–20} Therefore, HSCT interaction mediated by CB[8] is widely utilized in supramolecular self-assembly, and provides access to various assemblies, such as vesicles, hydrogels, and hierarchical nanoparticles.^{21,22} Presently, most of the widely used building blocks for supramolecular assembly are small molecules and polymers with different structures.^{23,24} Thus, it is highly desired to explore versatile building blocks for new applications of HSCT interaction.

From the point of view of structure, poly(ionic liquid)s (PILs), comprising ionic liquid units in their side chains or backbones, falls into the category of polyelectrolyte.^{25–28} However, PILs inherit some excellent performances deriving from ILs and polymers, such as wide electrochemical window, high ion conductivity, good processability, tunable structure, and polarity.^{29,30} Therefore, PILs have been rapidly developed since they were first reported by Ohno and Ito.³¹ In the previous studies, we have demonstrated a facile and universal one-step technique to prepare PIL-based nanogels, which can be achieved through the conventional free radical

Additional supporting information may be found in the online version of this article.

© 2019 Wiley Periodicals, Inc.

copolymerization of IL monomers and crosslinkers in selective solvent in the absence of stabilizers or surfactants.³² The structure and size of as-obtained PIL-based nanogels can be well regulated through changing the crosslinkers and IL monomers. In the light of broadly tunable structure of ILs, we also find that it is feasible to prepare stimuli-responsive PIL nanogels by introducing different functional groups into IL monomers. The as-formed PIL nanogels are of the stimuli responses including light, redox, temperature, and pH.^{33–35} Herein, novel PIL nanogel functionalized by naphthyl (Np) was synthesized via the as-reported one-step technique. Through using CB[8] as a host molecule, charge transfer interaction between PIL-nanogel and a bisviologen compound is achieved, which can be utilized to mediate supramolecular assembly of PIL nanogel (Fig. 1). To the best of our knowledge, HSCT complex using polymer nanogel as the building block has not yet been reported in the literatures.

EXPERIMENTAL

Materials

Azobisisobutyronitrile (AIBN, 98%) was recrystallized from methanol twice and stored in the fridge before use. To remove the inhibitors, vinyl imidazole (VIm), 4-vinylbenzyl chloride and ethylene glycol dimethacrylate (EGDMA) were distilled under vacuum and stored in the fridge. *N,N'*-dimethylformamide (DMF) was dried over calcium hydride overnight and distilled under reduced pressure. Dichloromethane (CH_2Cl_2) was dried over

calcium hydride for 4 h and distilled under normal pressure. IL monomers, 4-vinylbenzyl triphenyl phosphonium chloride (VBP-Ph), and 4-vinylbenzyltributyl phosphonium chloride (VBP-Bu) were prepared according to the reported protocols.^{32,33} Unless stated otherwise, all other reagents, such as triphenylphosphorus, tributylphosphorous, 2-naphthol, 4-chloro-1-butanol, *n*-hexane, methacryloyl chloride, 4,4'-bipyridine, 1,4-dibromobutane, amantadine (AdNH_2), carbamide, glyoxal solution (40 wt %) and methanol were A.R. grade and used as received without further treatment.

Characterization

Proton and carbon nuclear magnetic resonance (^1H and ^{13}C NMR) spectra were recorded on a Bruker AM spectrometer (400 MHz) at 25 °C. Mass spectrometric (MS) measurements were performed on an Agilent 6520 QTOF mass spectrometer equipped with electrospray ionization (ESI) source in positive and negative ion modes. Fourier transform infrared (FTIR) spectra were conducted on a DIGIL FTS3000 spectrophotometer using KBr tables. Ultraviolet-visible (UV-vis) absorption spectra were measured on a Shimadzu UV-2500PC spectrophotometer using a 1.0 cm path length quartz cell. Thermogravimetric analysis (TGA) were surveyed on a PerkinElmer TG/TGA 6300 at a heating rate of 10 °C/min. Dynamic light scattering (DLS) measurements were performed at 25 °C and a scattering angle of 90° on a commercial laser light scattering (ALV/SP-125) equipped with an ALV-5000

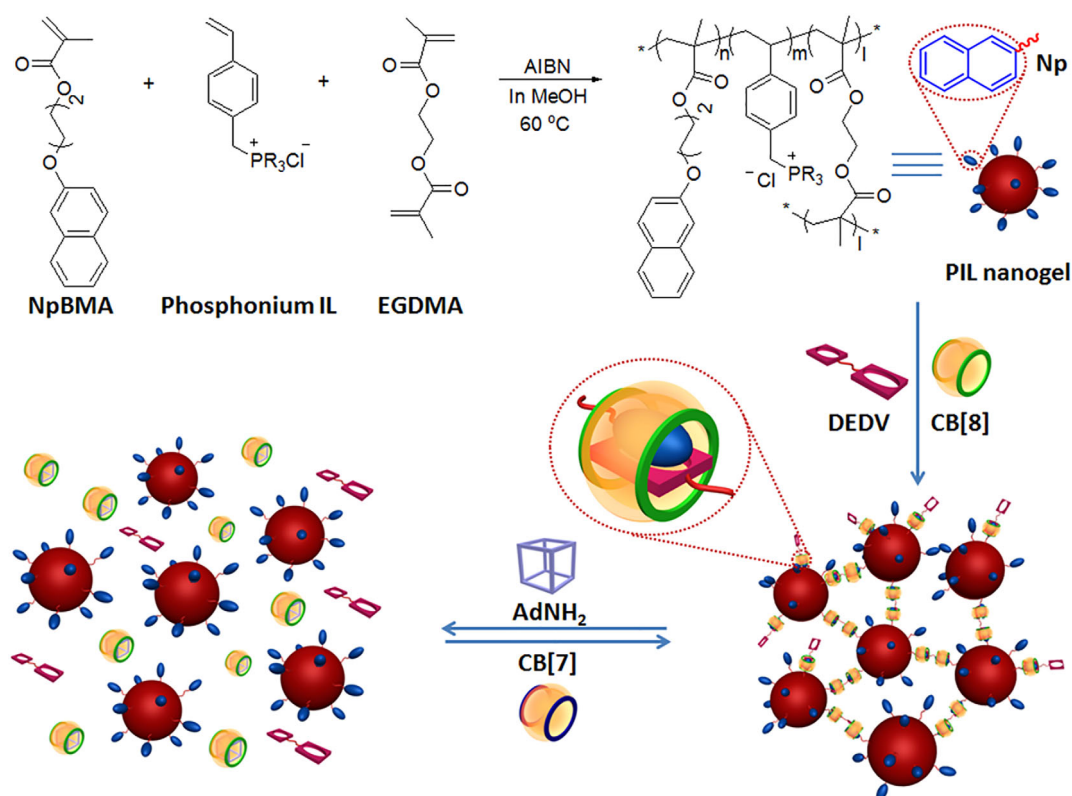


FIGURE 1 Schematically illustration of supramolecular assembly of PIL nanogel mediated by HSCT interaction. [Color figure can be viewed at wileyonlinelibrary.com]

multidigital time correlator and ADLAS DPY425 solid-state laser (output power = 22 mW at $\lambda = 632.8$ nm). The morphology of the samples was observed by scanning electron microscopy (SEM, JSM 6700F; Japan). The samples were prepared by directly dropping the dilute sample solution on the substrate. X-ray photoelectron spectroscopy (XPS) data were collected using a PerkinElmer PHI-5702 multifunctional XPS (Physical Electronics, Waltham, MA) with Al K_{α} radiation (1486.6 eV) as the excitation source. The adventitious carbon 1 s peak was calibrated at 285 eV and used as an internal standard to compensate for any charging effects.

Synthesis of 4-(Naphthalen-2-yloxy)butyl methacrylate

First, 4-hydroxybutyl-2-naphthyl ether (HBNp) was synthesized according to the reported protocol.³⁶ Typically, 2-naphthol (5.77 g, 40.02 mmol), 4-chloro-1-butanol (6.51 g, 59.96 mmol) and potassium carbonate (11.06 g, 80.0 mmol) were fed into a dried flask. Then, anhydrous DMF (50 mL) and potassium iodide (catalytic amount) were added into the above flask. The mixture was stirred at 80 °C for 30 h under nitrogen atmosphere. After cooling to room temperature, the reaction mixture was poured into deionized water (200 mL). White crude was obtained by filtration and purified by column chromatography using CH_2Cl_2 as eluent (retention factor R_f : 0.36). The product was obtained as a white powder (Yield: 1.31 g, 15.41%). mp: 106–109 °C. ^1H NMR (CDCl_3 , 400 MHz, δ ppm, Fig. S1): 7.79–7.69 (dd, 3H), 7.46–7.40 (t, 1H), 7.36–7.30 (t, 1H), 7.17–7.11 (d, 2H), 4.17–4.10 (t, 2H), 3.80–3.72 (t, 2H), 2.00–1.92 (m, 2H), 1.86–1.77 (m, 2H). ^{13}C NMR (CDCl_3 , 100 MHz, δ ppm, Fig. S2): 156.8, 134.5, 129.4, 128.9, 127.6, 126.7, 123.6, 118.9, 106.7, 67.7, 62.6, 29.6, 25.8. MS (ESI) m/z : calculated for $\text{C}_{14}\text{H}_{16}\text{O}_2$: 216.28, found: 216.16.

For the preparation of 4-(naphthalen-2-yloxy)butyl methacrylate (NpBMA), to a solution of HBNp (1.3 g, 6.0 mmol) and triethylamine (1.22 g, 12.0 mmol) in CH_2Cl_2 (30 mL), methacryloyl chloride (0.94 g, 8.99 mmol) in dried CH_2Cl_2 (10 mL) was added dropwise under stirring. The reaction mixture was kept below 0 °C for 1.0 h using ice-water bath. Then, it was further stirred at room temperature for 24 h. The reaction mixture was washed with saturated NaCl solution ($50 \times 3 \text{ mL}^2$). After that, the solution was dried over magnesium sulfate, and the solvent was removed through rotary evaporation. The crude product was further purified by column chromatography, using CH_2Cl_2 /petroleum ether as eluent (1:1, v/v, $R_f = 0.32$). The product was obtained as a light yellow liquid (Yield: 1.4 g, 72.51%). ^1H NMR (CDCl_3 , 400 MHz, δ

ppm, Fig. S3): 7.81–7.71 (m, 3H), 7.48–7.42 (t, 1H), 7.38–7.32 (t, 1H), 7.20–7.12 (m, 2H), 6.15 (s, 1H), 5.57 (s, 1H), 4.31–4.25 (t, 2H), 4.15–4.09 (t, 2H), 2.02–1.90 (m, 7H). ^{13}C NMR (CDCl_3 , 100 MHz, δ ppm, Fig. S4): 167.5, 156.9, 136.4, 134.6, 129.4, 129.0, 127.7, 126.7, 126.3, 125.4, 123.6, 118.9, 106.6, 67.3, 64.3, 26.0, 25.5, 18.3. MS (ESI) m/z : calculated for $\text{C}_{18}\text{H}_{20}\text{O}_3$: 284.35, found: 284.17.

Synthesis of 1,1'-(butane-1,4-diyl)bis(1-ethyl-4,4'-bipyridine-1,1'-diium)bromide (DEDV)

Compound **1** was synthesized according to the procedure described in the literature with a little modification (Fig. 2).¹³ 4-4'-Bipyridine (6.25 g, 40 mmol), 1,4-dibromobutane (2.87 g, 13 mmol) and acetonitrile (50 mL) were fed into a dried flask with a magnetic stirrer. The mixture was stirred at 70 °C for 24 h to produce a precipitate. The precipitate was then washed with acetonitrile (50 mL) and diethyl ether (50 mL) successively. A yellow powder was obtained and dried under vacuum (Yield: 5.24 g, 74.35%). ^1H NMR ($\text{DMSO}-d_6$, 400 MHz, δ ppm, Fig. S5): 9.24 (d, 4H), 8.85 (d, 4H), 8.65 (d, 4H), 8.02 (d, 4H), 4.70 (s, 4H), 2.03 (d, 4H). ^{13}C NMR ($\text{DMSO}-d_6$, 100 MHz, δ ppm, Fig. S6): 153.0, 151.7, 146.1, 141.5, 126.1, 122.6, 60.1, 27.8. MS (ESI) m/z : calculated for $\text{C}_{24}\text{H}_{28}\text{N}_4^{2+}$: 368.28, found: 368.26.

In the following step, Compound **1** (3.25 g, 6 mmol), bromoethane (2.68 g, 25 mmol) were dissolved in dried DMF (100 mL) and stirred at 90 °C for 48 h. The precipitate was obtained through filtration, and washed with hot DMF and acetonitrile ($30 \times 3 \text{ mL}^2$) to get a buff powder (Yield: 1.48 g, 33.16%). mp: 246–249 °C (decomposition). ^1H NMR ($\text{DMSO}-d_6$, 400 MHz, δ ppm, Fig. S7): 9.52–9.35 (m, 8H), 8.88–8.75 (m, 8H), 4.87–4.66 (m, 8H), 2.15–2.03 (d, 4H), 1.63–1.54 (t, 6H). ^{13}C NMR (D_2O , 100 MHz, δ ppm, Fig. S8): 145.4, 127.2, 126.9, 60.9, 27.3, 15.5. MS (ESI) m/z : calculated for $\text{C}_{28}\text{H}_{34}\text{N}_4^{4+}$: 426.21, found: 426.34.

Synthesis of cucurbit[8]uril (CB[8])

First, glycoluril was synthesized according to the literature (Fig. 3).³⁷ Typically, carbamide (18 g, 0.3 mol) was dissolved in distilled water (25 mL) in a flask. Then, H_2SO_4 (98%, 2.0 mL) was added slowly into the above solution. The solution was heated to 50 °C and glyoxal solution (40 wt %, 15.6 g, 0.11 mol) was added in 5 min using a constant pressure funnel. The temperature was kept at 85 °C for 2 h. After that, the reaction was stopped and the solution was cooled down to room temperature. Then, the solution was

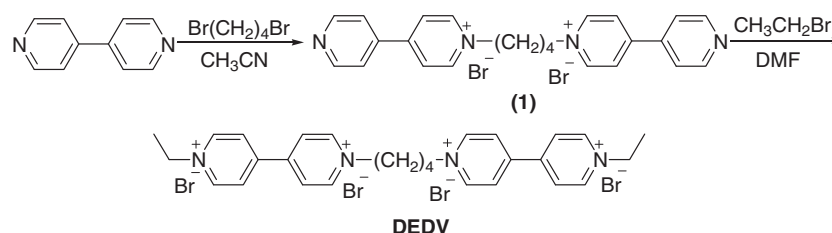


FIGURE 2 Synthesis of bisviologen compound DEDV.

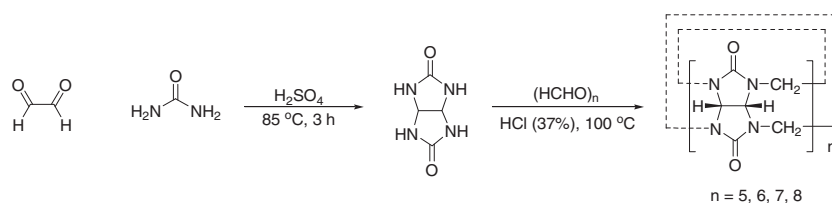


FIGURE 3 Synthesis of cucurbit[n]curls (CB[n]).

neutralized using NaOH solution (5.0 wt %). The precipitate was obtained through filtration and washed by distilled water. The product was dried under vacuum and obtained as white powder (Yield: 9.37 g, 60%). FTIR (Fig. S9): N–H (3300 cm^{-1} , st), C=O (1700 cm^{-1}), N–H (1500 cm^{-1} , ip; 800 cm^{-1} , oop), C–N (1300 cm^{-1} , st).

In the following step, glycoluril (155 g, 1.09 mol), paraformaldehyde (70 g, 2.33 mol), and concentrated hydrochloric acid (37 wt %, 800 mL) were mixed in a three-necked flask. The reaction was conducted at $100\text{ }^{\circ}\text{C}$ for 3 h. After that, the mixture was cooled down to room temperature. The precipitate (mixture of CB[5] and CB[8]) was collected by filtration. The resulting solution was concentrated and precipitated from substantial methanol (1000 mL). The as-obtained white solid (mixture of CB[6] and CB[7]) was collected through filtration, and washed with distilled water and acetone successively. The crude product (CB[5] and CB[8]) was dried under vacuum at $80\text{ }^{\circ}\text{C}$. In the next step, the mixture of CB[5] and CB[8] (100 g) was dissolved in hydrochloride (5 mol/L, 500 mL). The solution was boiled for 30 min (Be caution!). After that, the solution was cooled down to room temperature and white solid (CB[8]) was collected through filtration. The crude product (CB[8]) was dried under vacuum at $80\text{ }^{\circ}\text{C}$. The above manipulations were repeated four times until CB[8] with high purity (>95%, determined by ^1H NMR) was obtained. mp: $\sim 470\text{ }^{\circ}\text{C}$ (decomposition). ^1H -NMR (D_2SO_4 , 400 MHz, δ ppm, Fig. S10): 5.86–5.66 (d, 16H), 5.66–5.56 (s, 16H), 4.42–4.17 (d, 16H).

Preparation of Np-grafted PIL nanogels

Nanogels composed of different ILs were prepared according to our previous methods (Fig. 4).^{32,33} The following example describes the typical synthesis of Np-grafted PIL nanogels. NpBMA (0.107 g, 0.60 mmol), VBP-Ph (0.249 g, 0.60 mmol),

EGDMA (0.476 g, 2.40 mmol), and AIBN (0.009 g, 0.055 mmol) were dissolved in 30 mL absolute methanol, the mixture was stirred at $70\text{ }^{\circ}\text{C}$ for 40 h in nitrogen atmosphere. To remove the residual monomers, the as-prepared nanogel solutions were first dialyzed against methanol thoroughly. Then, nanogel solutions were further dialyzed against water. Finally, PIL-based nanogel powder was obtained by lyophilization. (Yield: 0.33 g, 40%). The as-prepared sample is defined as 1N1P4E, in which N, P, and E are short for NpBMA, VBP-Ph, and EGDMA, respectively, and the numbers are the feeding ratio of the corresponding monomers. The control sample 1P4E was prepared under the same conditions only without feeding NpBMA. To determine the concentration of PIL nanogels (calculated by Np group), Job's plot was measured through UV-vis at the absorbance of 328 nm using NpBMA solution in $\text{CH}_3\text{OH}:\text{H}_2\text{O}$ (3:1, v/v) as the samples. The fitted equation is $y = 14.88x - 0.04$ and the correlation coefficient R^2 is 0.9995.

RESULTS AND DISCUSSION

Preparation and characterization of Np-grafted PIL nanogel

First, Np group was introduced into methacrylate-based monomer (NpBMA). Its structure was confirmed by NMR, FTIR, and MS measurements. In addition, two phosphonium IL monomers, VBP-Ph and VBP-Bu, were synthesized and used as the comonomers. Subsequently, NpBMA was copolymerized with EGDMA in the presence of phosphonium IL monomers, which played the role of stabilizer in the polymerization process. As illustrated in Figure S15(A), opalescent solutions could be obtained under the above conditions. And there were no precipitates after the copolymerization reaction. Strong scattering light could be observed when the samples were illuminated by a laser pointer (650 nm). The performance demonstrates that there are many stable particles in the

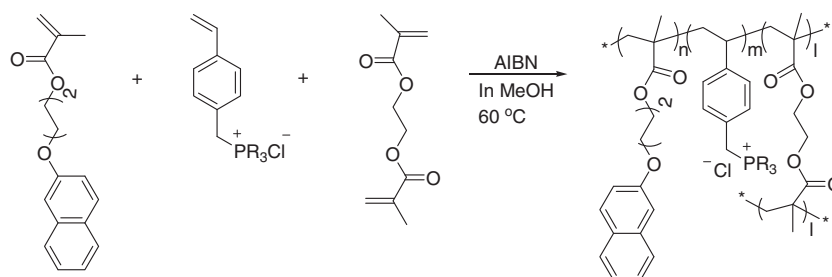


FIGURE 4 Synthesis of Np-grafted PIL nanogels ($R = \text{Bu}$ and Ph).

solution. Since the host-guest interaction will be conducted in water, the as-prepared Np-grafted PIL nanogel solutions were dialyzed against methanol and water successively, which could remove the unreacted monomers and exchange methanol with water. As shown in Figure S11(B), the strong scattering light confirms that Np-grafted PIL nanogels are still stable in water.

The sizes of Np-grafted PIL nanogel were measured through DLS and the results are summarized in Table 1. It can be found that the sizes of PIL nanogels are in the range of 50–130 nm. With increasing the feed of phosphonium IL monomer, PIL nanogel with smaller size can be obtained, which is probably because poly(phosphonium IL) segments play the role of stabilizer in the polymerization process. As a result, the size of Np-grafted PIL nanogel can be mediated through the feeding ratio of the monomers and the crosslinker. Similar to our previous studies, the sizes of PIL nanogels are still in a wide dispersity.^{34,35} DLS results also reveal that the substitution group in comonomers (VBP-Ph/Bu) has little influence on the size of Np-grafted PIL nanogel. In addition, the sizes of Np-grafted PIL nanogel become much larger after they are transferred into water through dialysis. It should be due to the stronger polarity of water than that of methanol, which will result in the association of PIL nanogel considering the presence of hydrophobic Np groups and PEGDMA segments. Another interpret is that water can partly shield the charges on the surface of PIL nanogels.

To confirm the presence of Np groups in PIL nanogel, UV-vis measurement was conducted. Before the measurement, the possible unreacted monomers in the as-prepared PIL nanogel solution were removed by dialysis against methanol thoroughly. Then, the solutions were further dialyzed against water to get PIL nanogel aqueous solution. Finally, Np-grafted PIL nanogel powders were obtained by freeze-drying. The monomer NpBMA was dissolved in the mixed solvent of methanol and water (3:1, v/v) as the control sample. As showed in

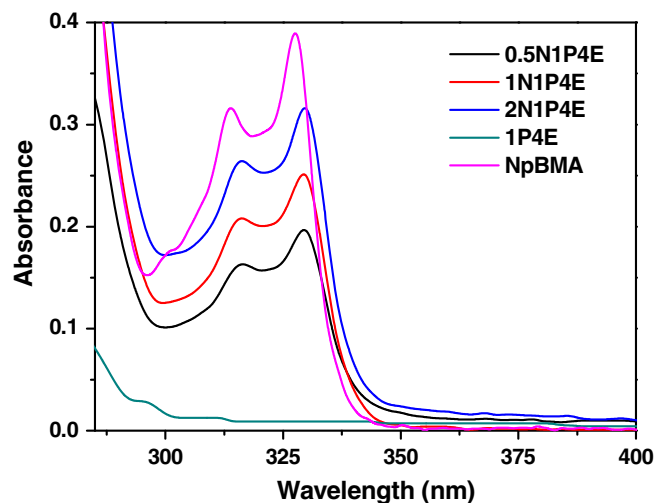


FIGURE 5 UV-vis spectra of PIL nanogels with different feeding ratios in water and NpBMA in CH₃OH:H₂O (3:1, v/v). [Color figure can be viewed at wileyonlinelibrary.com]

Figure 5, the strong absorption peaks at 313 nm and 327 nm are ascribed to the π - π^* transition of the naphthalene ring in NpBMA. Similar absorption peaks can be observed in PIL nanogels. The absorption enhances with increasing the feed of NpBMA monomer in the copolymerization. Compared with the typical absorption peaks in NpBMA, those in Np-grafted PIL nanogels redshift a little. This shift is probably ascribed to the difference in polarity between water and methanol. However, no absorptions can be observed in the above region in 1P4E, which is prepared in the absence of NpBMA monomer. Therefore, UV-vis results confirm the successful introduction of Np groups into PIL nanogel through the ternary copolymerization. The composition of PIL nanogels were also examined by XPS technique.

As revealed in Figure 6, PIL nanogel is mainly composed of carbon, oxygen, phosphorus, and chlorine besides hydrogen.

TABLE 1 Hydrodiameter and PDI of PIL Nanogels with Different Feeding Ratios Before and After Dialysis^a

Entry	Comonomer	Feeding ratio ^b	D_h (nm) ^c	PDI ^c	D_h (nm) ^d	PDI ^d
0.5N1P3E	VBP-Ph	0.5:1:3	130	0.34	159	0.59
0.5N1P4E	VBP-Ph	0.5:1:4	103	0.21	131	0.62
0.5N1P5E	VBP-Ph	0.5:1:5	83	0.32	113	0.71
1N1P4E	VBP-Ph	1:1:4	113	0.30	191	0.51
1N1P5E	VBP-Ph	1:1:5	87	0.48	162	0.32
1N1P6E	VBP-Ph	1:1:6	50	0.22	79	0.39
2N1P4E	VBP-Ph	2:1:4	122	0.42	236	0.42
2N1P5E	VBP-Ph	2:1:5	102	0.36	180	0.48
0.5N1B4E	VBP-Bu	0.5:1:4	114	0.46	160	0.65
1N1B4E	VBP-Bu	1:1:4	129	0.48	185	0.79

^a Polymerization conditions: ([EGDMA] + [NpBMA] + [Comonomer])/[AIBN] = 100:1, solvent: absolute methanol (30 mL), polymerization temperature = 70 °C. D_h , average hydrodynamic diameter; PDI, polydispersion index.

^b The molar ratio of NpBMA:[Comonomer]:EGDMA.

^c In methanol.

^d In water. In the abbreviation of samples, N, P/B, and E denote NpBMA, VBP-Ph/Bu, and EGDMA, respectively, and the numbers denote the molar feeding ratio of the corresponding monomers.

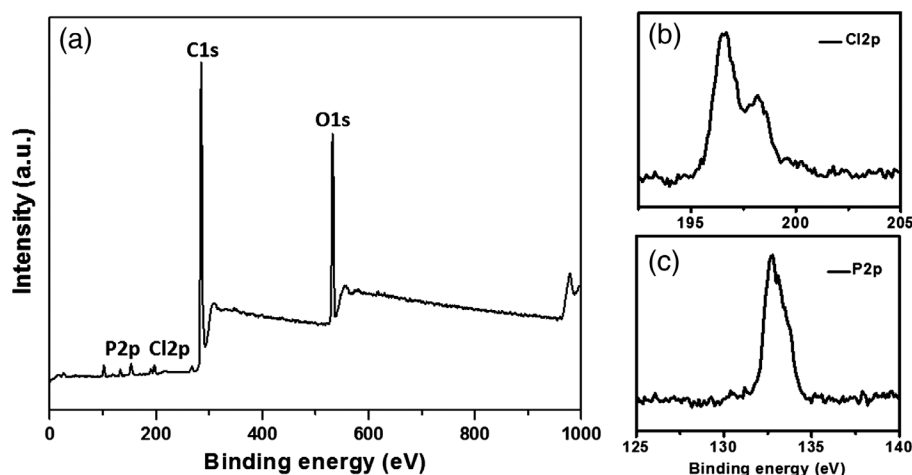


FIGURE 6 XPS survey spectrum of PIL nanogel (a) and the peaks of Cl2p (b) and P2p (c) orbits of PIL nanogel.

Both P and Cl come from phosphonium IL monomer. Thus, XPS data indicate that phosphonium IL monomers also participate in the ternary copolymerization.

FTIR spectra of the as-prepared PIL nanogels with various feeding ratios were recorded and exhibited in Figure 7. Some typical vibration peaks ascribed to the groups in PIL nanogels can be identified obviously, such as the peaks at 1720 and 1630 cm^{-1} , attributed to the stretching vibration of the carbonyl group and aromatic benzene ring. The peak ascribed to C—H bond (3054 cm^{-1} , stretching vibration) of the vinyl groups in the monomers disappeared after the crosslinking copolymerization. Therefore, FTIR results demonstrate that all monomers have participated in the ternary copolymerization, and Np containing PIL nanogels were produced.

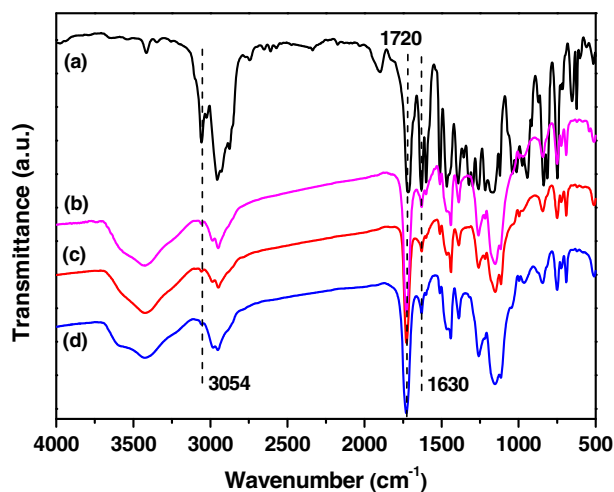


FIGURE 7 FTIR spectra of NpBMA and PIL nanogels with various feeding ratios. (a) NpBMA; (b) 0.5N1P4E; (c) 0.5N1P3E; and (d) 0.5N1P5E. All nanogel samples were prepared through lyophilization after dialysis against water. [Color figure can be viewed at wileyonlinelibrary.com]

Moreover, the thermostability of nanogels was determined by TGA. As shown in Figure S12, these PIL nanogels have good thermostability and are stable below 250 °C, due to the highly crosslinked structure. The slight weight loss before 150 °C was probably owing to the evaporation of retained solvents.

The morphologies of PIL nanogels were observed through SEM. As revealed in the images [Fig. 8(a,b)], the sizes of PIL nanogel are around 100 nm. These sizes are a little smaller than those measured by DLS, which is due to the absence of solvent in SEM measurement. In addition, PIL nanogel aggregate slightly after the solvent is removed. When PIL nanogel is transferred into water, they aggregate obviously judging from Figure 8(c,d). The results are consistent with DLS data, which probably results from the strong polarity of water that can shield the charges on the surface of PIL nanogel.

Supramolecular assembly of PIL nanogels driven by HSCT interaction

Since the charge transfer interaction between naphthalene and viologen group can be stabilized by the cavity of cucurbit [8]uril, tremendous host-guest supramolecular systems are fabricated through using versatile small molecules and polymers as the building blocks.³⁸ To achieve the supramolecular assembly of PIL nanogels, a bisviologen guest molecule (DEDV), which can be embedded into two equivalents of CB [8]'s cavities and act as a link, was synthesized through a two-step quaternization of viologen. Thereafter, HSCT supramolecular interaction was investigated by ¹H NMR using NpBMA as a model compound. As demonstrated in Figure 9, the signals of pyridinium hydrogens in DEDV emerge in the range from 8.5 to 9.2 ppm. After adding CB[8] into DEDV solution, the above signals show an upfield shift and become broader. The behavior reveals that there exists interaction between CB [8] and DEDV.³⁹ For the model molecule NpBMA, the signals at 7.1–7.8 ppm result from the protons in naphthalene group. When CB[8] and DEDV are introduced, the signals of Np proton in NpBMA show pronounced upfield shifts. Simultaneously, the signals of pyridinium protons in DEDV become

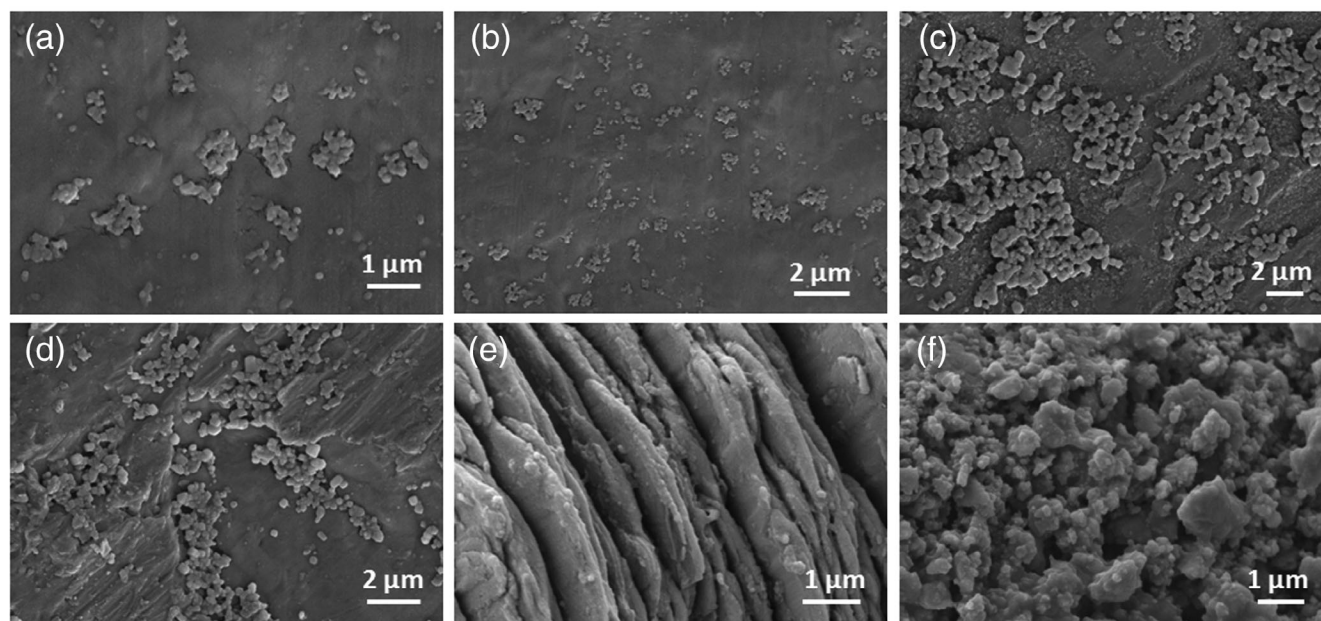


FIGURE 8 SEM images of PIL nanogels with different feeding ratios. (a) 1N1P5E in methanol; (b) 0.5N1P5E in methanol; (c) 1N1P5E in water; (d) 0.5N1P5E in water; (e) 0.5N1P4E + DEDV+CB[8] in water; and (f) 0.5N1P4E + DEDV+CB[8]+AdNH₂ in water.

much broader. Furthermore, the proton signals in Np and pyridinium exhibit a downfield shift when AdNH₂ is added into the above solution as a competitive guest. At the same time, these signals also become narrower. In view of the poor solubility of NpBMA, the signals resulting from Np group still

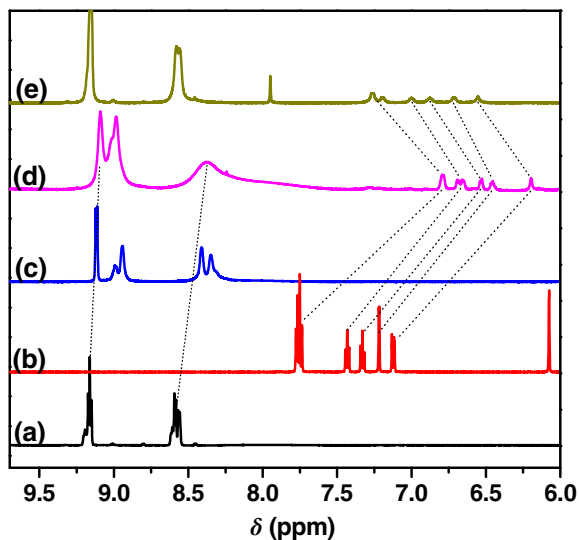


FIGURE 9 ¹H NMR spectra (400 MHz) of (a) DEDV in D₂O; (b) NpBMA in CD₃OD/D₂O (3/1, v/v); (c) DEDV + CB[8] in D₂O; (d) NpBMA + DEDV + CB[8] in D₂O; and (e) NpBMA + DEDV + CB[8] + AdNH₂ in D₂O. Concentrations: DEDV (3 mM), NpBMA (6 mM), CB[8] (6 mM), and AdNH₂ (6 mM). [Color figure can be viewed at wileyonlinelibrary.com]

keep broad. These performances further confirm that HSCT interaction can be achieved in the above ternary system, and can also be dissociated through introducing a competitive guest.

Afterward, Np-grafted PIL nanogels were complexed CB[8] and DEDV in water under stirring. It has been reported that CB[8] has very poor solvability in water, and can be only dissolved in water in the presence of strong acid. As shown in Figure 10, after adding DEDV and CB[8] into PIL nanogel solution, there are no CB[8] powders in the solution, and the clear solution becomes a stable milky emulsion. It has been demonstrated that the formation of charge transfer complex can greatly improve the solvability of CB[8] in water.⁴⁰ Therefore, the appearance of the solution shows the formation of ternary complex among CB[8], DEDV and PIL nanogel. In addition, the scattering light becomes much stronger after the addition of CB[8] and DEDV. It should be attributed to the aggregation of PIL nanogels due to the HSCT interaction. When AdNH₂ is introduced as a competitive guest molecule, the solution becomes clearer again. Since AdNH₂ is more affinitive to CB[8] than Np groups, HSCT complex among PIL nanogel, DEDV, and CB[8] will disassociate and form CB[8]-AdNH₂ complex. The existence of PIL nanogel can also be confirmed through the Tyndall effect. When CB[7] was added into the above system, the solution became opalescent. The behavior indicates the formation of HSCT complex again, which results from the stronger affinity of CB[7] to AdNH₂ than that of CB[8].⁴¹ Therefore, HSCT complex of CB[8], DEDV, and PIL nanogel can be recovered through introducing CB[7] as a competitive host molecule. It is found that all PIL nanogels can form HSCT

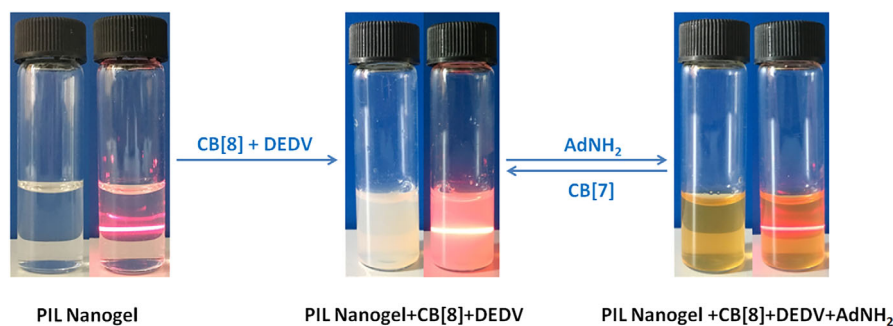


FIGURE 10 Photographs of association and dissociation of Np-grafted PIL-based nanogels. Concentrations: PIL nanogel (14 mM, calculated by Np group), CB[8] (14 mM), DEDV (7 mM), and AdNH₂ (14 mM). [Color figure can be viewed at wileyonlinelibrary.com]

interaction with DEDV in the presence of CB[8]. The structure of comonomers has no obvious influence on the interaction except for the size of PIL nanogels. Therefore, 0.5N1P4E was used in the following studies.

The size evolution of PIL nanogel during the process of HSCT interaction was monitored through DLS technique. As shown in Figure 11, the average size of 0.5N1P4E in water is 131 nm. When CB[8] was added into the solution, the size of PIL nanogel increases to 217 nm, which is probably due to the weak interaction between CB[8] and Np groups in PIL nanogel.⁴¹ After DEDV was added into the above solution, the average size of the particles increased to 755 nm. The size change is ascribed to the aggregation of PIL nanogels, which results from encapsulating Np groups in PIL nanogel and pyridine units in DEDV into the cavities of CB[8]. Since DEDV can act as links in the process, PIL nanogels accumulate together to form larger particles through the supramolecular interaction. In addition, the size of PIL nanogel aggregates decreased from 755 to 270 nm when AdNH₂ is added into the above solution. AdNH₂ is a competition guest molecule and has stronger affinity to CB[8] than Np. Therefore, Np units in CB

[8] cavity will be substituted by AdNH₂ and HSCT complexes are disassembled. The above size evolution can also be confirmed by SEM images. As illustrated in Figure 8(e), PIL nanogels aggregate and form schistose morphology in the scale of micrometer after the addition of DEDV and CB[8]. However, when AdNH₂ is introduced, the supramolecular complexes are dissociated and nanoparticles emerge [Fig. 8 (f)], indicating that AdNH₂ can break the HSCT interaction among CB[8], DEDV, and PIL nanogel.

HSCT interaction among Np-grafted PIL nanogel, DEDV, and CB[8] is further investigated through UV-vis measurement. Typically, the absorption band will have an obvious redshift (~100 nm) due to HSCT interaction.⁴² To confirm the HSCT interaction in CB[8]-DEDV-PIL nanogel ternary system, we used NpBMA as a model molecule. As illustrated in the curves of NpBMA and 0.5N1P4E (Fig. 12), there are no absorption bands above 400 nm. For the control sample CB[8]+DEDV, there are no obvious absorption peaks neither. However, when DEDV and CB[8] are added into NpBMA solution, there emerges strong absorption peaks above 400 nm, indicating

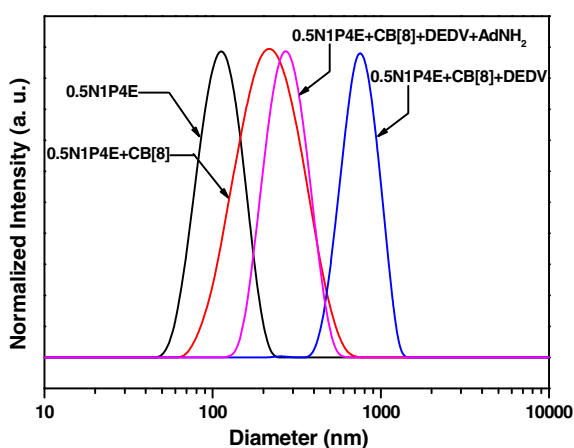


FIGURE 11 Size evolution of PIL nanogel in the process of HSCT interaction. Concentrations: 0.5N1P4E (2 mM, calculated by Np group), CB[8] (2 mM), DEDV (1 mM), and AdNH₂ (2 mM). [Color figure can be viewed at wileyonlinelibrary.com]

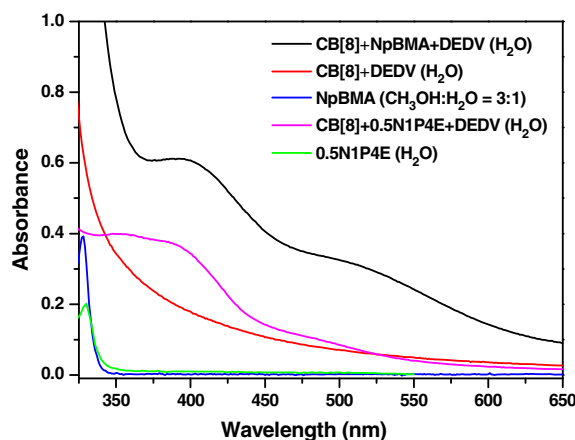


FIGURE 12 UV-vis spectra of CB[8] + DEDV, CB[8] + NpBMA + DEDV, CB[8] + 0.5N1P4E + DEDV, and NpBMA. Concentrations: 0.5N1P4E (2 mM, calculated by Np group), NpBMA (2 mM), CB [8] (2 mM), and DEDV (1 mM). [Color figure can be viewed at wileyonlinelibrary.com]

the formation of CT interaction between naphthalene ring and pyridine ring. For Np-grafted PIL nanogel sample (0.5N1P4E), there is also an absorption band around 400 nm after introducing CB[8] and DEDV. The above performance illustrates that there exists HSCT interaction between PIL nanogel and DEDV in the presence of CB[8].

CONCLUSIONS

Naphthyl functionalized PIL nanogels were facilely fabricated through one-step ternary crosslinking copolymerization in methanol. Considering the incorporation of phosphonium IL monomers, stable nanogel solutions with tunable size could be conveniently achieved through changing the feed ratio of IL monomer and the crosslinker EGDMA. As a result, the charge transfer interaction between Np group and DEDV molecules stabilized by CB[8] was accomplished. Since DEDV can act as the links, supramolecular assembly through HSCT interaction is successfully achieved by using PIL nanogels as the building blocks. In addition, the supramolecular aggregates of PIL nanogel can be dissociated by adding a competitive guest compound amantadine. Therefore, our studies provided a feasible strategy for the fabrication of dynamic nanoparticles, which has great potential applications in the smart material areas. However, there is still a limitation using PIL nanogel as the building block for host-guest interaction. That is, it is difficult to evaluate quantitatively the HSCT interaction due to the highly crosslinked structure of PIL nanogel.

ACKNOWLEDGMENT

This work was supported by the National Natural Science Foundation of China (Project Nos. 21774101 and 21474080).

REFERENCES AND NOTES

- 1 A. Das, S. Ghosh, *Angew. Chem. Int. Ed.* **2014**, *53*, 2038.
- 2 P. Wei, X. Yan, F. Huang, *Chem. Soc. Rev.* **2015**, *44*, 815.
- 3 E. Busseron, Y. Ruff, E. Moulin, N. Giuseppone, *Nanoscale* **2013**, *5*, 7098.
- 4 X. Y. Hu, T. Xiao, C. Lin, F. Huang, L. Wang, *Acc. Chem. Res.* **2014**, *47*, 2041.
- 5 J. Hu, G. Zhang, Z. Ge, S. Liu, *Prog. Polym. Sci.* **2014**, *39*, 1096.
- 6 Z. Z. Tong, J. Y. Zhou, R. S. Huang, J. Zhou, R. K. Zhang, W. Q. Zhuo, G. H. Jiang, *J. Polym. Sci. Part A: Polym. Chem.* **2017**, *55*, 2477.
- 7 C. Stoffelen, J. Voskuhl, P. Jonkheijm, J. Huskens, *Angew. Chem. Int. Ed.* **2014**, *53*, 3400.
- 8 Q. D. Hu, H. Fan, Y. Ping, W. Q. Liang, G. P. Tang, J. Li, *Chem. Commun.* **2011**, *47*, 5572.
- 9 T. C. Liang, I. H. Chiang, P. J. Yang, D. Kekuda, C. W. Chu, H. C. Lin, *J. Polym. Sci. Part A: Polym. Chem.* **2009**, *47*, 5998.
- 10 R. Y. M. Zhang, Y. H. Liu, Y. Liu, *Adv. Mater.* **2019**, 1806158. <https://doi.org/10.1002/adma.201806158>.
- 11 H. Yao, J. X. Wang, X. Song, H. T. Zhang, X. D. Fan, W. Tian, *Acta Polym. Sin.* **2017**, *48*, 63.
- 12 Z. W. Ji, J. F. Li, G. S. Chen, M. Jiang, *ACS Macro Lett.* **2016**, *5*, 588.
- 13 Y. Liu, Y. Yu, J. Gao, Z. Wang, X. Zhang, *Angew. Chem. Int. Ed.* **2010**, *49*, 6576.
- 14 H. D. Correia, S. Chowdhury, A. P. Ramos, L. Guy, G. J. F. Demets, C. Bucher, *Polym. Int.* **2019**, *68*, 572.
- 15 X. L. Ni, X. Xiao, H. Cong, Q. J. Zhu, S. F. Xue, Z. Tao, *Acc. Chem. Res.* **2014**, *47*, 1386.
- 16 C. S. Y. Tan, J. del Barrio, J. Liu, O. A. Scherman, *Polym. Chem.* **2015**, *6*, 7652.
- 17 U. Rauwald, O. A. Scherman, *Angew. Chem. Int. Ed.* **2008**, *47*, 3950.
- 18 H. J. Kim, J. Heo, W. S. Jeon, E. Lee, J. Kim, S. Sakamoto, K. Yamaguchi, K. Kim, *Angew. Chem. Int. Ed.* **2001**, *40*, 1526.
- 19 K. Kim, *Chem. Soc. Rev.* **2002**, *31*, 96.
- 20 Y. Liu, R. Fang, X. Tan, Z. Wang, X. Zhang, *Chem. A Eur. J.* **2012**, *18*, 15650.
- 21 Y. Xu, M. Guo, X. Li, A. Malkovskiy, C. Wesdemiotis, Y. Pang, *Chem. Commun.* **2011**, *47*, 8883.
- 22 Y. H. Ko, K. Kim, J. K. Kang, H. Chun, J. W. Lee, S. Sakamoto, K. Yamaguchi, J. C. Fettinger, K. Kim, *J. Am. Chem. Soc.* **2004**, *126*, 1932.
- 23 J. del Barrio, P. N. Horton, D. Lairez, G. O. Lloyd, C. Toprakcioglu, O. A. Scherman, *J. Am. Chem. Soc.* **2013**, *135*, 11760.
- 24 Z. W. Ji, J. H. Liu, G. S. Chen, M. Jiang, *Polym. Chem.* **2014**, *5*, 2709.
- 25 J. Yuan, D. Mecerreyes, M. Antonietti, *Prog. Polym. Sci.* **2013**, *38*, 1009.
- 26 W. Qian, J. Texter, F. Yan, *Chem. Soc. Rev.* **2017**, *46*, 1124.
- 27 J. Illescas, M. Casu, V. Alzari, D. Nuvoli, M. A. Scorciapino, R. Sanna, V. Sanna, A. Mariani, *J. Polym. Sci. Part A: Polym. Chem.* **2014**, *52*, 3521.
- 28 A. S. Shaplov, D. O. Ponkratov, Y. S. Vygodskii, *Polym. Sci. Series B* **2016**, *58*, 73.
- 29 Y. Men, D. Kuzmicz, J. Yuan, *Curr. Opin. Colloid Interface Sci.* **2014**, *19*, 76.
- 30 M. M. Obadia, S. Fagour, Y. S. Vygodskii, F. Vidal, A. Sergehi, A. S. Shaplov, E. Drockenmuller, *J. Polym. Sci. Part A: Polym. Chem.* **2016**, *54*, 2191.
- 31 H. Ohno, K. Ito, *Chem. Lett.* **1998**, *27*, 751.
- 32 Y. Xiong, H. Wang, R. Wang, Y. Yan, B. Zheng, Y. Wang, *Chem. Commun.* **2010**, *46*, 3399.
- 33 Y. Zuo, J. Yu, X. Liu, P. Cao, P. Song, R. Wang, Y. Xiong, *Polym. Chem.* **2017**, *8*, 1146.
- 34 Y. Xiong, J. Liu, Y. Wang, H. Wang, R. Wang, *Angew. Chem. Int. Ed.* **2012**, *51*, 9114.
- 35 Y. Zuo, N. Guo, Z. Q. Jiao, P. F. Song, X. Liu, R. M. Wang, Y. B. Xiong, *J. Polym. Sci. Part A: Polym. Chem.* **2016**, *54*, 169.
- 36 E. A. Appel, F. Biedermann, U. Rauwald, S. T. Jones, J. M. Zayed, O. A. Scherman, *J. Am. Chem. Soc.* **2010**, *132*, 14251.
- 37 J. Kim, I. S. Jung, S. Y. Kim, E. Lee, J. K. Kang, S. Sakamoto, K. Yamaguchi, K. Kim, *J. Am. Chem. Soc.* **2000**, *122*, 540.
- 38 Y. H. Ko, K. Kim, E. Kim, K. Kim, *Supramol. Chem.* **2007**, *19*, 287.
- 39 G. X. Liu, Y. M. Zhang, C. H. Wang, Y. Liu, *Chem. A Eur. J.* **2017**, *23*, 14425.
- 40 F. Biedermann, M. Vendruscolo, O. A. Scherman, A. De Simone, W. M. Nau, *J. Am. Chem. Soc.* **2013**, *135*, 14879.
- 41 H. Chen, H. Yang, W. Xu, Y. Tan, *RSC Adv.* **2013**, *3*, 13311.
- 42 Y. H. Ko, E. Kim, I. Hwang, K. Kim, *Chem. Commun.* **2007**, 1305.